EPJ manuscript No.
(will be inserted by the editor)

Oscillatory nonequilibrium Nambu systems: the canonical-dissipative Yamaleev oscillator

S. Mongkolsakulvong[1], P. Chaikhan[1], T.D. Frank[2,3,4,*]

[1]Faculty of Science, Department of Physics, Kasetsart University, Bangkok 10900, Thailand
[2]Center for the Ecological Study of Perception and Action, Department of Psychology, University of Connecticut, 406 Babbidge Road, Storrs, CT 06269, USA
[3]Systems Biology Ireland, University College Dublin, Belfield, Dublin 4, Ireland
[4]UCD School of Physics, University College Dublin, Belfield, Dublin 4, Ireland

Received: date / Revised version: date

Abstract. We study the emergence of oscillatory self-sustained behavior in a nonequilibrium Nambu system that features an exchange between different kinetical and potential energy forms. To this end, we study the Yamaleev oscillator in a canonical-dissipative framework. The bifurcation diagram of the nonequilibrium Yamaleev oscillator is derived and different bifurcation routes that are leading to limit cycle dynamics and involve pitchfork and Hopf bifurcations are discussed. Finally, an analytical expression for the probability density of the stochastic nonequilibrium oscillator is derived and it is shown that the shape of the density function is consistent with the oscillator properties in the deterministic case.

PACS. 05.45.-a Nonlinear dynamics – 05.40.Jc Brownian motion – 05.70.Ln Nonequilibrium thermodynamics

1 Introduction

In a seminal paper, Nambu introduced a generalization of Hamiltonian dynamics [1] — nowadays called Nambu mechanics. Nambu mechanics describes the evolution of a N-dimensional system with state vector $\mathbf{r} = (r_1, \ldots, r_N)$ that satisfy N-1 integrals of motion $H_1(\mathbf{r}), \ldots, H_{N-1}(\mathbf{r})$. Consequently, the system under consideration evolves on a 1-dimensional manifold in the N-dimensional state space. Explicitly, the evolution equation of such a system is given by

$$\frac{\mathrm{d}}{\mathrm{d}t} r_k(t) = \sum_{i_1,\ldots,i_{N-1}} \epsilon_{k,i_1,\ldots,i_{N-1}} \frac{\partial H_1}{\partial r_{i_1}} \cdots \frac{\partial H_{N-1}}{\partial r_{i_{N-1}}} \ , \quad (1)$$

where t denotes time and $\epsilon_{k,i_1,\ldots,i_{N-1}}$ is the N-dimensional epsilon tensor (Levi-Civita tensor). Importantly, for a three-dimensional system with state vector $\mathbf{r} = (r_1, r_2, r_3)$ and invariants H_1 and H_2 Eq. (1) reduces to

$$\frac{\mathrm{d}}{\mathrm{d}t}\mathbf{r} = \nabla H_1(\mathbf{r}) \times \nabla H_2(\mathbf{r}) \quad (2)$$

with $\nabla = (\partial/\partial r_1, \partial/\partial r_2, \partial/\partial r_3)$. For a two-dimensional system with state vector $\mathbf{r} = (r_1, r_2)$ exhibiting just one invariant of motion $H(\mathbf{r})$, Nambu mechanics reduces to Hamiltonian mechanics (i.e., Eq. (1) becomes)

$$\frac{\mathrm{d}}{\mathrm{d}t} r_1 = \frac{\partial H}{\partial r_2} \ , \quad \frac{\mathrm{d}}{\mathrm{d}t} r_2 = -\frac{\partial H}{\partial r_1} \ . \quad (3)$$

Nambu mechanics applies to a variety of interesting dynamical systems, see Table 1. For example, using Eq. (2) rigid body rotations have been studied in the framework of Nambu mechanics [1–6]. Particles moving on curved surfaces (e.g., spheres) have been described by Nambu equations that can be cast into the form of Eq. (1), see Refs. [7–10]. Certain electrodynamic [5,11–15] and biochemical [16,17] problems have been re-formulated using the multi-Hamiltonian approach of Nambu mechanics. Multi-Hamiltonian oscillators generalizing the harmonic oscillator [18,19], chiral models [8] and the Calogero-Moser system [20,21] have been studied in the context of Nambu mechanics.

While one key benefit of Nambu mechanics is that it provides us with a principled way to construct evolution equations from invariants of motion, this benefit also limits the applicability of Nambu's multi-Hamiltonian approach to systems that features such invariants. However, problems in interdisciplinary research fields such as biophysics frequently address nonequilibrium systems and are dissipative in nature. Consequently, they often require a generalization of the classical concept of invariants of

* Corresponding author: T. D. Frank; e-mail: till.frank@uconn.edu, till.frank@ucd.ie

Table 1. Conservative classical Nambu systems studied in the literature

Systems	Reference
Rigid-body rotation	[1–6]
Motion on a sphere	[7–10]
Electrodynamic systems	[5, 11–15]
Multi-Hamiltonian oscillators (Yamaleev)	[18, 19]
Chiral models	[8]
Calogero-Moser model	[20, 21]

motion. For example, in order to study swarm dynamics and animal mobility we need to consider agents that take up energy from the environment and/or exhibit energy depots. In this context, the theoretical framework of active Brownian particles [22] and canonical-dissipative systems [23–25] has been developed not only to address swarm behavior [26,27] but also animal mobility and self-propagation in general [28–30]. Much of this research has been inspired by Lord Rayleigh's early work on nonlinear oscillators with velocity-dependent friction [31]. The question arises whether Nambu mechanics can be generalized to take dissipative phenomena into account that typically occur in nonequilibrium systems — just as this has been done in the aforementioned studies for Hamiltonian mechanics. Similarly, we may ask whether in the context of Nambu mechanics a counterpart to the nonlinear Rayleigh oscillator can be found. The first question has been answered in the affirmative in two recent studies [32, 33]. However, so far, only two examples of dissipative, oscillatory Nambu systems have been studied: particles spinning around on a sphere [32] and rigid-body rotations [33]. Both types of oscillatory systems are qualitatively different from limit cycle oscillators. Consequently, the second question related to Nambu limit cycle oscillators has not yet been addressed. As a step in the direction of developing a broader scope of dissipative, nonequilibrium Nambu systems including limit cycle oscillators, we will focus on a generalization of the harmonic oscillator suggested by Yamaleev [18,19] that can be cast into the form of Eq. (2).

The Yamaleev oscillator is an important Nambu system because (as opposed to Nambu rotator systems) the Yamaleev oscillator involves a generalized restoring force. Moreover, the oscillator yields certain insights into oscillations subjected to anharmonic potential forces and for appropriately chosen initial conditions the Yamaleev oscillator describes solutions of the relativistic harmonic oscillator. We will return briefly to these issues in Sec. 4.

2 Yamaleev oscillator

The Yamaleev oscillator is defined on a three-dimensional state space that is spanned by one spatial coordinate x and two kinetical variables v_1 and v_2 that might be regarded as generalized velocities. Let $\mathbf{r} = (x, v_1, v_2)$ denote the state vector. Then, the oscillator dynamics is given by Eq. (2), where H_1 and H_2 are Hamiltonian-like functions defined by [18,19,34]

$$H_1 = \frac{v_1^2 + ax^2}{2} \tag{4}$$

and

$$H_2 = \frac{v_2^2 + ax^2}{2} \tag{5}$$

with $a > 0$. Note that in what follows we use the nabla operator $\nabla = (\partial/\partial x, \partial/\partial v_1, \partial/\partial v_2)$. From Eq. (2) it follows that the oscillator equations in components are given by

$$\begin{aligned} \frac{\mathrm{d}}{\mathrm{d}t}x &= v_1 v_2 \ , \\ \frac{\mathrm{d}}{\mathrm{d}t}v_1 &= -axv_2 \ , \\ \frac{\mathrm{d}}{\mathrm{d}t}v_2 &= -axv_1 \ . \end{aligned} \tag{6}$$

A key property of the oscillator dynamics (6) and of any Nambu system in general is that the Hamiltonian functions are invariants of the dynamics. That is, from Eq. (2) it follows that H_1 and H_2 as functions of time are constants. For graphical illustration purposes it is useful to introduce re-scaled variables: $u_1 = v_1/\sqrt{a}$ and $u_2 = v_2/\sqrt{a}$. Substituting these variables into the Hamiltonian functions (4) and (5), we obtain

$$H_1 = \frac{a}{2}\left(u_1^2 + x^2\right) \tag{7}$$

and

$$H_2 = \frac{a}{2}\left(u_2^2 + x^2\right) \ . \tag{8}$$

Note that in what follows we will use the state space (x, u_1, u_2) for illustration purposes only. All analytical considerations will be carried out in the original (x, v_1, v_2) space.

There are two types of solutions. Fixed point solutions $\mathrm{d}x/\mathrm{d}t = \mathrm{d}v_1/\mathrm{d}t = \mathrm{d}v_2/\mathrm{d}t = 0$ and oscillatory solutions. Oscillatory solutions can be graphically determined by exploiting the two invariants H_1 and H_2. That is, let us consider an oscillatory solutions with $H_1 = c_1 > 0$ and $H_2 = c_2 > 0$. Then, we have in the space (x, u_1, u_2) the constraints $u_1^2 + x^2 = 2c_1/a$ and $u_2^2 + x^2 = 2c_2/a$, see Eqs. (7) and (8). Consequently, oscillatory solutions can be found on the intersections of two cylinders. More precisely, we have one cylinder orientated along the u_2 axis with radius $r_1 = \sqrt{2c_1/a}$, see Fig. 1. The other cylinder is orientated along the u_1 axis and has radius $r_2 = \sqrt{2c_2/a}$, see Fig. 2. For $r_1 \neq r_2$ the two cylinder intersect on two closed orbits, see Fig. 3. These orbits describe periodic solutions of the Yamaleev oscillator (6). Fig. 4 depicts an oscillatory solution that corresponds to one of the two intersects shown in Fig. 3. The trajectories $x(t)$, $v_1(t)$ and $v_2(t)$ shown in Fig. 4 were computed from Eq. (6) by means of an Euler forward simulation scheme.

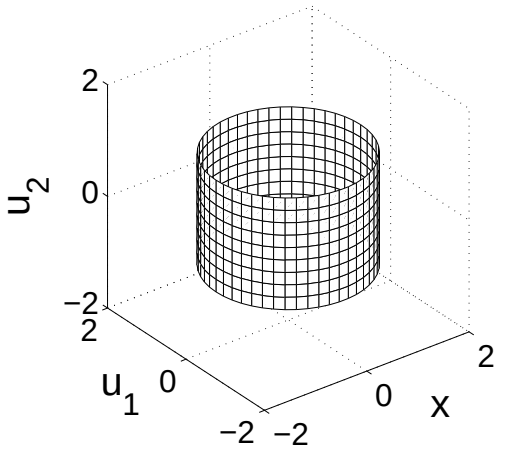

Fig. 1. Cylinder with axis in the direction of u_2 and radius r_1 in the plane (u_1, x). All possible trajectories on the cylinder surface satisfy the conditions $H_1 = \text{constant}$. Here $r_1 = \sqrt{2} \approx 1.4$.

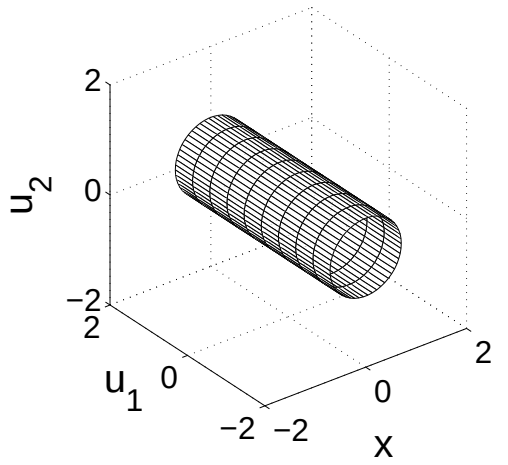

Fig. 2. Cylinder with axis in the direction of u_1 and radius r_2 in the plane (u_2, x). All possible trajectories on the cylinder surface satisfy the conditions $H_2 = \text{constant}$. Here $r_2 = \sqrt{0.5} \approx 0.7$.

3 Canonical-dissipative, nonequilibrium Yamaleev oscillator

Following [32,33], we consider a canonical-dissipative generalization of the Yamaleev oscillator (2). To this end, we introduce the function g describing the potential of a dissipative force $-\nabla_D\, g$ that accounts both for pumping and damping. The incomplete nabla operator is defined by $\nabla_D = (0, \partial/\partial v_1, \partial/\partial v_2)$ and makes sure that the dissipative force only acts on the kinetical variables v_1 and v_2.

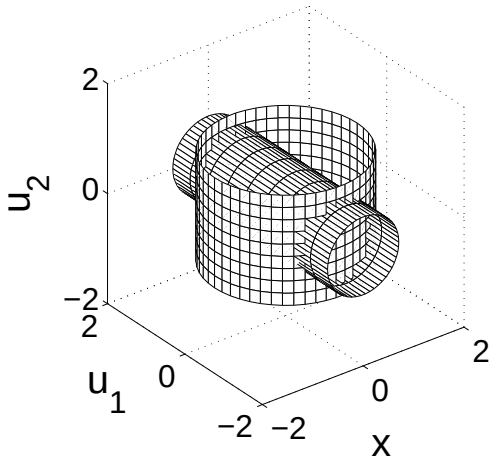

Fig. 3. Illustration of the intersection of the two cylinders shown in Figs. 1 and 2. The two intersections describe two oscillatory solutions of the Yamaleev oscillator (6). That is, they describe two closed trajectories for which H_1 and H_2 are invariant over time.

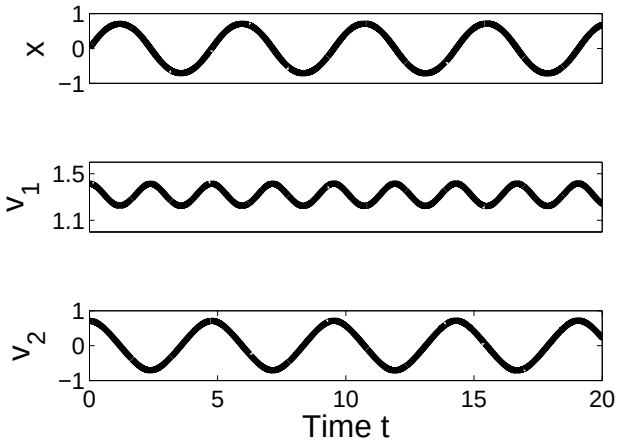

Fig. 4. Oscillatory solution of the Yamaleev oscillator (6) computed numerically using an Euler forward iterative scheme. Single time step: $\Delta t = 0.001$. Parameters: $a = 1$. Initial values: $x(0) = 0$, $v_1 = r_1 = \sqrt{2}$ (see Fig. 1), $v_2 = r_2 = \sqrt{0.5}$ (see Fig. 2).

In detail, we put

$$g(x, v_1, v_2) = \frac{\gamma}{2}\left[(H_1(x, v_1) - b_1)^2 + (H_2(x, v_2) - b_2)^2\right], \tag{9}$$

where b_1 and b_2 are constants that can assume both positive or negative values. The parameter $\gamma > 0$ describes the overall strength of the dissipative force and defines for $b_1, b_2 > 0$ the overall characteristic time-scale on which the Hamiltonian functions H_1 and H_2 decay to their stationary values (see [32,33] and below). The dissipative pumping and damping mechanisms are related to the presence

of fluctuating forces affecting the oscillator dynamics. Just as in the case of the dissipative force $-\nabla_D\, g$, we will consider only fluctuating force acting directly on the kinetic variables v_1 and v_2. To this end, we use the incomplete unit matrix E_D defined by

$$E_D = \begin{pmatrix} 0\,0\,0 \\ 0\,1\,0 \\ 0\,0\,1 \end{pmatrix} \ . \tag{10}$$

The total fluctuating force is then given by the vector $\sqrt{Q}E_D \cdot \mathbf{\Gamma}(t)$ with $\mathbf{\Gamma}(t) = (\Gamma_1(t), \Gamma_2(t), \Gamma_3(t))$, where $\Gamma_i(t)$ are statistically independent Langevin forces normalized to 2 (for details see [35]) and $Q \geq 0$ is the overall amplitude of the fluctuating force (noise amplitude). Adding the dissipative force $-\nabla_D\, g$ and the fluctuating force $\sqrt{Q}E_D \cdot \mathbf{\Gamma}(t)$ to the oscillator dynamics (2), we obtain

$$\frac{\mathrm{d}}{\mathrm{d}t}\mathbf{r} = \nabla H_1 \times \nabla H_2 - \nabla_D g + \sqrt{Q}E_D \cdot \mathbf{\Gamma}(t) \ . \tag{11}$$

It is useful to write Eq. (11) in components:

$$\begin{aligned} \frac{\mathrm{d}}{\mathrm{d}t}x &= v_1 v_2 \ , \\ \frac{\mathrm{d}}{\mathrm{d}t}v_1 &= -axv_2 - \gamma\ v_1(H_1 - b_1) + \sqrt{Q}\Gamma_2(t) \ , \\ \frac{\mathrm{d}}{\mathrm{d}t}v_2 &= -axv_1 - \gamma\ v_2(H_2 - b_2) + \sqrt{Q}\Gamma_3(t) \ . \end{aligned} \tag{12}$$

3.1 Deterministic case

In what follows, we consider the deterministic case for $Q = 0$. That is, we consider the oscillator dynamics defined by

$$\frac{\mathrm{d}}{\mathrm{d}t}\mathbf{r} = \nabla H_1 \times \nabla H_2 - \nabla_D g \ , \tag{13}$$

which reads in components

$$\begin{aligned} \frac{\mathrm{d}}{\mathrm{d}t}x &= v_1 v_2 \ , \\ \frac{\mathrm{d}}{\mathrm{d}t}v_1 &= -axv_2 - \gamma v_1\,(H_1 - b_1) \ , \\ \frac{\mathrm{d}}{\mathrm{d}t}v_2 &= -axv_1 - \gamma v_2\,(H_2 - b_2) \ . \end{aligned} \tag{14}$$

3.1.1 Behavior in the long time limit (asymptotic case)

Since $g \geq 0$ this implies that in the long time limit $t \to \infty$ we have $\mathrm{d}g/\mathrm{d}t = 0$. Consider $\mathrm{d}g/\mathrm{d}t$ in the case of $Q = 0$:

$$\frac{\mathrm{d}}{\mathrm{d}t}g = -\gamma^2((H_1 - b)^2 v_1^2 + (H_2 - b)^2 v_2^2) \leq 0 \tag{15}$$

Since $\nabla_D\, g = (0, \gamma v_1(H_1 - b), \gamma v_2(H_2 - b))$, we have $(\nabla_D g)^2 = \nabla_D\, g \cdot \nabla_D\, g = 0 + (\gamma v_1(H_1 - b))^2 + (\gamma v_2(H_2 - b))^2$. Thus Eq. (15) becomes

$$\frac{\mathrm{d}}{\mathrm{d}t}g = -(\nabla_D\, g)^2 \ . \tag{16}$$

In the case of $\mathrm{d}g/\mathrm{d}t = 0$ Eq. (16) implies $\nabla_D\, g = 0$. Then from Eq. (13) it follows that in the long time limit we have the conservative Yamaleev dynamics (2). Consequently, we are dealing with fixed point solutions and oscillatory solutions. How do they depend on the parameters b_1 and b_2? In order to answer this question, we first study the evolution of the Hamiltonian functions H_1 and H_2. Consider $\mathrm{d}H_1/dt$:

$$\frac{\mathrm{d}}{\mathrm{d}t}H_1 = v_1\frac{\mathrm{d}}{\mathrm{d}t}v_1 + ax\frac{\mathrm{d}}{\mathrm{d}t}x \ . \tag{17}$$

Recall that for $Q = 0$ we have $\mathrm{d}v_1/\mathrm{d}t = -axv_2 - \gamma(H_1 - b_1)v_1$ and $\mathrm{d}x/\mathrm{d}t = v_1 v_2$. Substituting these terms into Eq. (17), we obtain

$$\frac{\mathrm{d}}{\mathrm{d}t}H_1 = -\gamma v_1^2(H_1 - b_1) \ . \tag{18}$$

For the auxiliary variable $L_1 = (H_1 - b_1)^2/2$ we find $\mathrm{d}L_1/\mathrm{d}t = -2\gamma v_1^2 L_1 \leq 0$. Similarly for H_2 we get $\mathrm{d}H_2/\mathrm{d}t = -\gamma v_2^2(H_2 - b_2)$ and for $L_2 = (H_2 - b_2)^2/2$ we find $\mathrm{d}L_2/\mathrm{d}t = -2\gamma v_2^2 L_2 \leq 0$. Since $L_1, L_2 \geq 0$ and $\mathrm{d}L_1/\mathrm{d}t, \mathrm{d}L_2/\mathrm{d}t \leq 0$ holds, the functions L_1 and L_2 are Lyapunov functions. It follows that L_1, L_2 become stationary in the long time limit, which implies that H_1 and H_2 become stationary as well.

3.1.2 Existence and stability of oscillatory solutions

First of all, from Eq. (6) it follows that oscillatory solutions do not exist if $v_1 = 0$ or $v_2 = 0$ for all times $t > t^*$, where t^* is an arbitrary reference time point. Second, for $b_1 \leq 0$ the function L_1 exhibits only one minimum at $H_1 = 0$. Consequently, if we do not have $v_1 = 0$ for $t > t^*$, then from $\mathrm{d}L_1/\mathrm{d}t = -2\gamma v_1^2 L_1 \leq 0$ it follows that we have $H_1 \to 0$ in the long term limit. However, in this case v_1 must converge to zero. Consequently, for $b_1 \leq 0$ the canonical-dissipative system (13) either exhibits solutions with $v_1 = 0$ or converges to solutions with $v_1 = 0$. The same argument applies to the parameter b_2: if $b_2 \leq 0$ then we either have $v_2 = 0$ for $t > t^*$ or the velocity v_2 converges to zero. In sum, if $b_1 \leq 0$ or $b_2 \leq 0$ holds then the canonical-dissipative oscillator (13) cannot exhibit oscillatory solutions. In contrast, for $b_1 > 0$ and $b_2 > 0$, the general stationarity condition $\nabla_D g = 0$ and the more specific stationarity conditions $\mathrm{d}L_1/\mathrm{d}t = \mathrm{d}L_2/\mathrm{d}t = 0$ are satisfied for $H_1 = b_1$ and $H_2 = b_2$. In this case oscillatory solutions exist as demonstrated in Sec. 2 (see in particular Fig. 3). In the Nambu system (2,...,5) all oscillatory solutions are neutrally stable. That is, perturbations persist. In contrast, as we will show below, the canonical-dissipative oscillator (15) can exhibit oscillatory solutions that correspond to stable limit cycles for $b_1 > 0 \wedge b_2 > 0$.

The canonical-dissipative oscillator (15) exhibits stable limit cycles if all fixed points with $v_1 = v_2 = 0$ are unstable. The reason for this is that for $b_1 > 0 \wedge b_2 > 0$ the functions L_1 and L_2 have minima at $H_1 = b_1$ and $H_2 = b_2$, respectively. If the dynamics (13) is not trapped in a fixed point with $v_1 = v_2 = 0$ (i.e., if any fixed point with

Table 2. Parameter domains and fixed points

Case	Conditions	Fixed points
I	$b_1 \leq 0 \wedge b_2 \leq 0$	$(x,0,0)$
II	$b_1 > 0 \wedge b_2 \leq 0$	$(x,0,0)$, $(0,\pm\sqrt{2b_1},0)$
III	$b_1 \leq 0 \wedge b_2 > 0$	$(x,0,0)$, $(0,0,\pm\sqrt{2b_2})$
IV	$b_1 > 0 \wedge b_2 > 0$	$(x,0,0)$, $(0,\pm\sqrt{2b_1},0)$, $(0,0,\pm\sqrt{2b_2})$

$v_1 = v_2 = 0$ is unstable) then for $t \to \infty$ the Hamiltonian-like functions H_1 and H_2 approach the fixed point energy values b_1 and b_2, respectively. This in turn implies that the trajectory x, v_1, v_2 approaches an oscillatory solution defined graphically in the three-dimensional (x, v_1, v_2) state space by an two-tori-intersection, see Fig. 3. The oscillatory solution corresponding to such a two-tori-intersection then represents a stable limit cycle. Consequently, in order to show the existence of stable limit cycles for $b_1 > 0 \wedge b_2 > 0$ we need to study next the existence and the stability of the fixed points.

3.1.3 Existence of fixed point solutions

We consider the existence of fixed points in the general case. That is, we consider the conditions listed in Table 2. In order to determine the fixed points, we put $\mathrm{d}\mathbf{r}/\mathrm{d}t = 0$ in Eq. (14):

$$\begin{aligned} 0 &= v_1 v_2 \ , \\ 0 &= axv_2 + \gamma v_1 \left(H_1(x,v_1) - b_1\right) \ , \\ 0 &= axv_1 + \gamma v_2 \left(H_2(x,v_2) - b_2\right) \ . \end{aligned} \tag{19}$$

Furthermore, we note that H_1 and H_2 need to be stationary. From Eq. (18) and the fact that $H_1 \geq 0$ we obtain the following conditions:

$$b_1 \leq 0 \Rightarrow v_1 = 0 \ , \ b_1 > 0 \Rightarrow v_1 = 0 \ \vee \ H_1 = b_1 \ . \tag{20}$$

Likewise, from $\mathrm{d}H_2/\mathrm{d}t = -\gamma v_2^2 (H_2 - b_2) = 0$ and $H_2 \geq 0$ it follows that

$$b_2 \leq 0 \Rightarrow v_2 = 0 \ , \ b_2 > 0 \Rightarrow v_2 = 0 \ \vee \ H_2 = b_2 \ . \tag{21}$$

Let us exploit these relations in combination with Eq. (19). First of all, we see that in any case the origin $(x, v_1, v_2) = (0,0,0)$ is a fixed point. In case I of Table 2 from Eqs. (20) and (21) it follows $v_1 = v_2 = 0$. We see that in case I the point $(x, v_1 = 0, v_2 = 0)$ is a fixed point solution of Eq. (19) for arbitrary x and includes the origin as special case. There are no other fixed point solutions. In other words, the whole x-axis represent a family of fixed points. In case II from Eq. (21) it follows that $v_2 = 0$. We then distinguish between two sub-cases. We can have $v_1 = 0$ as well. Then $(x, v_1 = 0, v_2 = 0)$ is a fixed point solution of Eq. (19) again. Alternatively, there are fixed point solutions with $v_1 \neq 0$. If $v_1 \neq 0$ and $v_2 = 0$ then from Eq. (19c) it follows that $x = 0$. Furthermore, from Eq. (19b) it follows that $H_1 = b_1$, which gives us $v_1 = \pm\sqrt{2b_1}$. That is, the dynamical system exhibits a fixed point $(x = 0, v_1 = \pm\sqrt{2b_1}, v_2 = 0)$. There are no other fixed points. Case III can be treated by analogy. The fixed points are $(x, v_1 = 0, v_2 = 0)$ and $(x = 0, v_1 = 0, v_2 = \pm\sqrt{2b_2})$. Finally, in case IV by substituting $(x, v_1 = 0, v_2 = 0)$ into Eq. (19) we see that the points on the x-axis are fixed points again. The remaining three possible sub-cases can be classified in terms of the pairs $(v_1 \neq 0, v_2 = 0)$, $(v_1 = 0, v_2 \neq 0)$, and $(v_1 \neq 0, v_2 \neq 0)$. For $(v_1 \neq 0, v_2 = 0)$ we repeat the argument made in case II and see that $(x = 0, v_1 = \pm\sqrt{2b_1}, v_2 = 0)$ is a fixed points. Likewise, for $(v_1 = 0, v_2 \neq 0)$ we follow the argument made in case III and see that $(x = 0, v_1 = 0, v_2 \pm \sqrt{2b_2})$ is a fixed points. The sub-case $(v_1 \neq 0, v_2 \neq 0)$ does not yield a stationary solution because of Eq. (19a). Table 2 summarizes the fixed points of the oscillator.

3.2 Stability of fixed point solutions and oscillatory solutions

3.2.1 Overview

In this section we examine the stability of fixed point and oscillatory solutions. Table 3 anticipates the results. The proofs follow below. From the results summarized in Table 3 it follows that in case I only the origin $(0,0,0)$ is marginally stable. The remaining points on the x-axis are unstable with respect to perturbations that move them away from the x-axis and neutrally stable with respect to perturbations that keep them on the x-axis. In cases II and III only $(0,\pm\sqrt{2b_1}),0)$ and $(0,0,\pm\sqrt{2b_2})$, respectively, are asymptotically stable fixed points. The points on the x-axis including the origin are unstable. In case IV all fixed points are unstable. Only oscillatory solutions represent stable limit cycles. In particular, for $b_1 < b_2$ the fixed points $(0,\pm\sqrt{2b_1},0)$ act as centers from which oscillatory solutions bifurcate, whereas for $b_2 < b_1$ oscillatory solutions bifurcate from the fixed points $(0,0,\pm\sqrt{2b_1})$, see also Sec. 3.2.3.

3.2.2 Proofs

For the fixed point $(0,0,0)$ we linearize Eq. (14) at the origin. For the variables v_1 and v_2 we obtain

$$\frac{\mathrm{d}}{\mathrm{d}t} v_1 = \gamma b_1 v_1 \ , \ \frac{\mathrm{d}}{\mathrm{d}t} v_2 = \gamma b_2 v_2 \ . \tag{22}$$

Consequently, if $b_1 < 0$ and $b_2 < 0$ the perturbations in the two-dimensional subspace (v_1, v_2) decay such that $v_1, v_2 \to 0$ for $t \to \infty$. Furthermore, from Eq. (18) which in our context reads $\mathrm{d}H_1/\mathrm{d}t = -\gamma v_1^2 (H_1 + |b_1|)$ and its counterpart $\mathrm{d}H_2/\mathrm{d}t = -\gamma v_2^2 (H_2 + |b_2|)$ it follows that $H_1 \to 0$ (if $v_1(0) \neq 0$) or $H_2 \to 0$ (if $v_2(0) \neq 0$) for $t \to \infty$ which in turn implies that $x \to 0$ for $t \to \infty$. These considerations hold for perturbations away from the x-axis (i.e. we have after the perturbation the initial condition $v_1(0) \neq 0 \vee v_2(0) \neq 0$). Any perturbation of the fixed point

Table 3. Stability analysis summary (Lin. = linear stability analysis; NL = nonlinear analysis; Lyap. = Lyapunov's direct method; stable* = neutrally stable for perturbations along x-axis and asymptotically stable for all other perturbations; unstable* = neutrally stable for perturbations along the x-axis and unstable for all other perturbations; unstable** = neutrally stable for perturbations along the x-axis but there exist other perturbations for which the fixed point is unstable)

Fixed points, limit cycles	Method	Condition/Stability
$(0,0,0)$	NL	$b_1<0 \wedge b_2<0 \Rightarrow$ stable*
	Lin.	$b_1>0 \vee b_2>0 \Rightarrow$ unstable*
$(x\neq 0,0,0)$	NL	$b_1<0 \vee b_2<0 \Rightarrow$ unstable**
	NL	$b_1>0 \wedge b_2>0$ and $b_1\neq b_2 \Rightarrow$ unstable**
	Lin.	$b_1>0 \wedge b_2>0$ and $b_1=b_2 \Rightarrow$ unstable**
$(0,\pm\sqrt{2b_1},0)$	Lin.	$b_1>0 \wedge b_2<0 \Rightarrow$ stable
		$b_1>0 \wedge b_2>0 \Rightarrow$ unstable
$(0,0,\pm\sqrt{2b_2})$	Lin.	$b_1<0 \wedge b_2>0 \Rightarrow$ stable
		$b_1>0 \wedge b_2>0 \Rightarrow$ unstable
limit cycle solutions	Lyap. method	$b_1>0 \wedge b_2>0 \Rightarrow$ stable

$(0,0,0)$ in the direction to another fixed point $(x\neq 0,0,0)$ does not decay. In sum, our nonlinear analysis shows that in the case $b_1<0 \wedge b_2<0$ the origin $(0,0,0)$ is neutrally stable for perturbations in the direction of the x-axis and is asymptotically stable for all other perturbations. Furthermore, from Eq. (22) it follows that the linear stability analysis is sufficient to show that the fixed point $(0,0,0)$ is unstable for $b_1>0 \vee b_2>0$ (cf. also Table 3). Again, these considerations only apply to perturbations that shift the origin away from the x-axis. Perturbations along the x-axis persists. Therefore, for $b_1>0 \vee b_2>0$ the origin is neutrally stable with respect to perturbations along the x-axis and unstable with respect to all other perturbations.

As shown in Sec. 3.1.3 all points $(x\neq 0,0,0)$ on the x-axis are fixed points. Consequently, perturbations of these fixed points along the x-axis are neutrally stable. Next, we consider perturbations that shift a fixed point $(x\neq 0,0,0)$ out of the x-axis such that after the perturbations we have $v_1(0)\neq 0$ and/or $v_2(0)\neq 0$. For $b_1<0 \vee b_2<0$ it follows from Eq. (18) and its counterpart $\mathrm{d}H_2/\mathrm{d}t=-\gamma v_2^2(H_2-b_2)$ that (i) we have $H_1\to 0$ if $b_1<0$ and we choose a perturbation with $v_1(0)\neq 0$ or (ii) $H_2\to 0$ if $b_2<0$ and we consider a perturbation with $v_2(0)\neq 0$. Let us consider the case $b_1<0$ (the case $b_2<0$ can be treated by analogy). Then we choose a perturbation such that the perturbed Hamiltonian $H_1(0)$ is smaller than the unperturbed $H_1=ax^2/2$. That is, we choose $v_1(0)\neq 0$ and $x(0)\neq x$ such that $v_1(0)^2/2+ax(0)^2/2<ax^2/2$. Since we have $\mathrm{d}H_1/\mathrm{d}t<0$ the function H_1 cannot increase. In other words, H_1 cannot approach the unperturbed function value $H_1=ax^2/2$. This implies that the system cannot return to the fixed point $(x\neq 0,0,0)$: the fixed point $(x\neq 0,0,0)$ is unstable. The case $b_1>0\wedge b_2>0$ is discussed in the appendix 5.1. The detailed analysis carried out there shows that for $b_1>0\wedge b_2>0$ the fixed point $(x\neq 0,0,0)$ is unstable as well.

Next, let us determine the stability of the fixed point $(0,\pm\sqrt{2b_1},0)$ by means of linear stability analysis. To this end, we consider $x(t)\approx 0$ and $v_2(t)\approx 0$ such that both variables are of magnitude ϵ, where ϵ is a small quantity. In this case, the term xv_2 in Eq. (14b) is a small quantity of second order in ϵ. Likewise, the term $v_1H_1=v_1(v_1^2+ax^2)/2$ involves the expression $av_1x^2/2$, which corresponds to a small quantity of second order in ϵ. Neglecting these terms, from Eq. (14b) we obtain

$$\frac{\mathrm{d}}{\mathrm{d}t}v_1=-\gamma v_1\left(\frac{v_1^2}{2}-b_1\right) . \tag{23}$$

We still need to linearize this relation with respect to v_1. We substitute $v_1(t)=\epsilon(t)\pm\sqrt{2b_1}$ into Eq. (23), where ϵ is small. Then, the linearized evolution equation for ϵ reads

$$\frac{\mathrm{d}}{\mathrm{d}t}\epsilon=-2\gamma b_1\,\epsilon . \tag{24}$$

Consequently, the perturbation ϵ decays to zero in the long time limit. Next, we substitute $v_1(t)=\epsilon(t)\pm\sqrt{2b_1}$, $x(t)\approx 0$, and $v_2(t)\approx 0$ into Eqs. (14a) and (14c) in order to obtain linearized evolution equations for $x(t)$ and $v_2(t)$. We obtain

$$\frac{\mathrm{d}}{\mathrm{d}t}x=Cv_2 , \quad \frac{\mathrm{d}}{\mathrm{d}t}v_2=-aCx+\gamma b_2v_2 \tag{25}$$

with $C=\pm\sqrt{2b_1}$. We see that these evolution equation do not depend on ϵ. That is, the three-dimensional (x,ϵ,v_2) state spaces decouples into the two-dimensional state space (x,v_2) and the ϵ dynamics. Eq. (25) can equivalently be expressed as second-order differential equation

$$\frac{\mathrm{d}^2}{\mathrm{d}t^2}x=\gamma b_2\frac{\mathrm{d}}{\mathrm{d}t}x-aC^2x . \tag{26}$$

For $b_2<0$ we are dealing with an damped oscillator and $x(t)$ (and consequently $v_2(t)$) approach zero in the long time limit. Consequently, the fixed point $(0,\pm\sqrt{2b_1},0)$ is stable for $b_2<0$. In contrast, for $b_2>0$ the oscillator exhibits a negative damping term. That is, the oscillation amplitude increases with time. This implies that the fixed point in the subspace (x,v_2) represents an unstable focus for $b_2>0$. In short, in the original space (x,v_1,v_2) the fixed point $(0,\pm\sqrt{2b_1},0)$ is unstable for $b_2>0$.

The stability of the fixed point $(0,0,\pm\sqrt{2b_2})$ can be determined in analogy to the previous case. Consequently, for $b_1<0$ the fixed point is stable, whereas for $b_1>0$ the fixed point is unstable.

Finally, for sake of completeness, let us summarize our arguments made in sections 3.1.1 and 3.1.2 concerning the existence and stability of limit cycle solutions. In the long time limit, by means of Lyapunov's direct method, it can be shown that the functions g, H_1, and H_2 become stationary, see Sec. 3.1.1. In the stationary case, the canonical-dissipative force defined by $-\nabla_D\,g$ equals zero and we are dealing with the Nambu system (2,. . . ,5) that can exhibit

fixed points and oscillatory solutions. Consequently, in the long term limit the dynamics of the canonical-dissipative system (15) either converges to a fixed point or settles down in an oscillatory solution. For $b_1, b_2 > 0$ limit cycle solutions exist, see Sec. 3.1.2. Graphically, these oscillatory solutions are given as intersections of two tori, see Fig. 3. There a two oscillatory solutions that in general are spatially separated from each other. More precisely, for $b_2 < b_1$ ($b_1 < b_2$) we have one oscillatory solution with $v_1 > 0$ ($v_2 > 0$) and another for $v_1 < 0$ ($v_2 < 0$). Moreover, as shown in this section, for $b_1, b_2 > 0$ all fixed point solutions are unstable. Consequently, the canonical-dissipative system (15) can only settle down into an oscillatory solution. Any perturbation of such an oscillatory solution cannot result in a bifurcation to a fixed point behavior. Rather, the dynamic system must return to the oscillatory solution. Consequently, the oscillator solution represents a stable limit cycle.

3.2.3 Bifurcation diagram

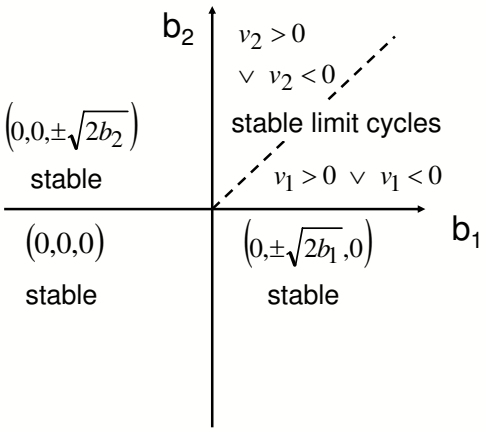

Fig. 5. Bifurcation diagram of the canonical-dissipative Yamaleev oscillator defined by Eq. (14). See text for details.

The bifurcation diagram of the nonequilibrium Yamaleev oscillator in the parameter space spanned by b_1 and b_2 is shown in Fig. 5. Accordingly, for $b_1, b_2 < 0$ the oscillator exhibits a stable fixed point at the origin. If we cross the b_2-axis for $b_2 < 0$, i.e., increase b_1 from negative to positive values, then there is a pitchfork bifurcation that makes the origin unstable, see Fig. 6 (top panel). The stable fixed points $(0, \sqrt{2b_1}, 0)$ and $(0, -\sqrt{2b_1}, 0)$ emerge. If subsequently, we cross the b_1-axis for $b_1 > 0$ then the stable fixed points $(0, \sqrt{2b_1}, 0)$ and $(0, -\sqrt{2b_1}, 0)$ become unstable foci and stable limit cycle emerge (Hopf bifurcation). Figure 7 shows a simulation of this bifurcation route (for $a = 1$). For $t < 20$ we have $b_1 = r_1/2 = 1 > 0$ and $b_2 < 0$. At $t = 20$ we switch b_2 from $b_2 < 0$ to $b_2 = r_2/2 = 0.25$. The oscillatory behavior emerges. The stable limit cycle corresponds again to the two-tori intersection with $u_1 > 0$ shown in Fig. 3. Consequently, the oscillatory trajectories shown in Fig. 7 evolve on the same limit cycle as the trajectories shown in Fig. 4. Note that in order to calculate the trajectories in Fig. 7 we solved the stochastic model (12) for a relatively weak noise source $Q = 0.001$ by using an stochastic Euler forward scheme [35]. Let us return to the bifurcation diagram shown in Fig. 5. Let us again consider first the parameter domain $b_1, b_2 < 0$ involving the origin $(0, 0, 0)$ as stable fixed point. If we cross the b_1 axis for $b_1 < 0$ by increasing b_2 from negative to positive values, then the canonical-dissipative system (14) exhibits again a pitchfork bifurcation. The origin becomes unstable and the stable fixed points $(0, 0, \sqrt{2b_2})$ and $(0, 0, -\sqrt{2b_2})$ emerge, see Fig. 6 (bottom panel). If we scale next b_1 from negative to positive values, then these fixed points become unstable foci and two stable limit cycles emerge. In short, there are two different routes that connect the parameter domain $b_1, b_2 < 0$ exhibiting the origin as stable fixed point with the parameter domain $b_1, b_2 > 0$ exhibiting stable limit cycles.

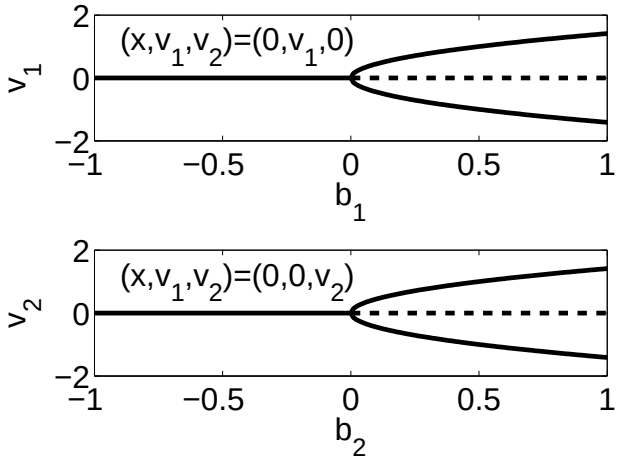

Fig. 6. Top panel: pitchfork bifurcation occurring for $b_2 < 0$ when b_1 is scaled beyond zero. Bottom panel: pitchfork bifurcation occurring for $b_1 < 0$ when b_2 is scaled beyond zero.

3.3 Stochastic case

Let us address briefly the stochastic case $Q > 0$. The Langevin equation (11) corresponds to the Fokker-Planck equation [33],

$$\frac{\partial}{\partial t} P = -\nabla \cdot \{\mathbf{I} P - (\nabla_D \; g)\, P\} + Q \Delta_D P \qquad (27)$$

with the divergencefree force

$$\mathbf{I} = \nabla H_1 \times \nabla H_2 \; . \qquad (28)$$

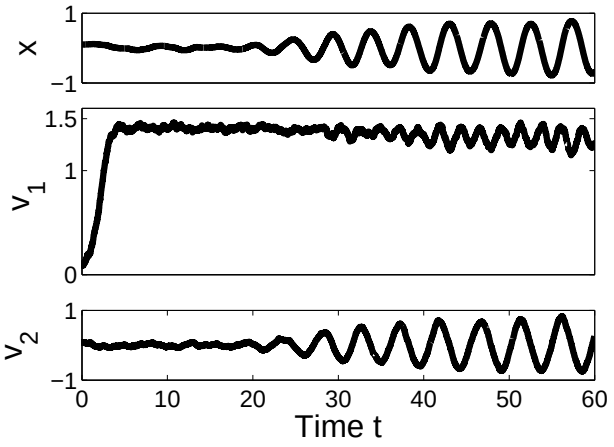

Fig. 7. Simulation of the dynamics of the canonical-dissipative oscillator (14). For $t < 20$ we used $b_1 = 1$ and $b_2 = -1$. The dynamics converges to the fixed point $(0, \sqrt{2b_1}, 0)$. At $t = 20$ we switched b_2 from $b_2 = -1$ to $b_2 = 0.25$. The limit cycle behavior emerged. Solutions of Eq. (14) were actually calculated under the impact of a weak fluctuating force. That is, $x(t)$, $v_1(t)$, and $v_2(t)$ were computed from Eq. (12) for $Q = 0.001$ (Euler forward scheme with time step $\Delta t = 0.01$). Fixed parameter: $a = 1$.

Eq. (27) determines the evolution of the probability density $P(x, v_1, v_2, t)$. In Eq. (27) the operator Δ_D is the incomplete Laplace operator defined by $\Delta_D = \partial^2/\partial v_1^2 + \partial^2/\partial v_2^2$. Eq. (27) is a special case of the Fokker-Planck equation for canonical-dissipative Nambu systems proposed in an earlier study [33]. Accordingly, the stationary (i.e., time-independent) probability density assumes the form

$$P(x, v_1, v_2) = \frac{1}{Z} \exp\left\{-\frac{g(H_1, H_2)}{Q}\right\} \tag{29}$$

with $Z = \int \exp\{-g(H_1, H_2)/Q\}\, \mathrm{d}x\, \mathrm{d}v_1\, \mathrm{d}v_2$ (normalization constant). Let us show explicitly that Eq. (29) solves Eq. (27). First, note that the right-hand side of Eq. (27) reads explicitly

$$RHS = -\nabla \cdot (\mathbf{I}P) + \nabla \cdot \{(\nabla_D\, g)\, P\} + Q\Delta_D P\ . \tag{30}$$

Second, note that the operator relation $\nabla_D \cdot \nabla_D$ is equivalent to $\nabla \cdot \nabla_D$ which implies that $\Delta_D = \nabla \cdot \nabla_D$. With this relation at hand, for the distribution (29) the diffusion term (Q-term) in the expression RHS yields

$$Q\Delta_D P = Q\nabla \cdot (\nabla_D P) = Q\nabla \cdot (P\, \nabla_D\, g)\ . \tag{31}$$

Substituting this result into Eq. (30), we see that the terms involving g cancel such that Eq. (30) becomes

$$\mathrm{RHS} = -\nabla \cdot (\mathbf{I}P) = -\underbrace{(\nabla \cdot \mathbf{I})}_{=0} P - \mathbf{I} \cdot \nabla P = -\mathbf{I} \cdot \nabla P\ . \tag{32}$$

As indicated above, we have exploited the fact that the force $\mathbf{I}$ has zero divergence. For ∇P we obtain

$$\nabla P = -\frac{P}{Q}\nabla g = -\frac{P}{Q}\left(\frac{\partial g}{\partial H_1}\nabla H_1 + \frac{\partial g}{\partial H_2}\nabla H_2\right)\ . \tag{33}$$

Using Eq. (33), we see that the scalar product $\mathbf{I} \cdot \nabla P$ equals zero because we have $\mathbf{I} \cdot \nabla H_1 = 0$ and $\mathbf{I} \cdot \nabla H_2 = 0$ (hint: see the definition of $\mathbf{I}$ in Eq. (28)).

Let us examine next some analytical properties of the stationary probability density (29) of the Fokker-Planck equation (27). Substituting Eq. (9) into Eq. (29), we find that the stationary probability density is explicitly given by

$$P(x, v_1, v_2) = \frac{1}{Z} \exp\left\{-\frac{\gamma}{2Q}\left([H_1(x, v_1) - b_1]^2 + [H_2(x, v_2) - b_2]^2\right)\right\}\ , \tag{34}$$

where H_1 and H_2 are defined by Eqs. (4) and (5). Using Eq. (33), we compute the gradient of P:

$$\nabla P = -\frac{\gamma P}{Q}\left\{[H_1(x, v_1) - b_1]\begin{pmatrix} ax \\ v_1 \\ 0 \end{pmatrix} + [H_2(x, v_2) - b_2]\begin{pmatrix} ax \\ 0 \\ v_2 \end{pmatrix}\right\}\ . \tag{35}$$

For case I (see Table 2) we are interested in determining the gradient of P at the origin. From Eq. (35) it follows that

$$\nabla P|_{(0,0,0)} = \begin{pmatrix} 0 \\ 0 \\ 0 \end{pmatrix}\ . \tag{36}$$

The vanishing gradient indicates that for case I (i.e., $b_1 < 0 \wedge b_2 < 0$) the probability density P has a maximum at the origin. Likewise, for case II the gradient at the stable case-II-fixed-points $(0, \pm\sqrt{2b_1}, 0)$ vanishes. More precisely, from Eq. (35) and $H_1 - b_1 = 0$ for $(x, v_1, v_2) = (0, \pm\sqrt{2b_1}, 0)$ it follows that

$$\nabla P|_{(0,\pm\sqrt{2b_1},0)} = \begin{pmatrix} 0 \\ 0 \\ 0 \end{pmatrix}\ . \tag{37}$$

Again, this indicates that the probability has two peaks at these fixed points. By analogy, in case III the probability density has maxima at the fixed points $(0, 0, \pm\sqrt{2b_2})$. In order to address the oscillatory case, we compute the Lie derivative of P. In our context, the Lie derivative $\mathbf{L}$ is given by the operator $\mathbf{I} \cdot \nabla$. We see that

$$\mathbf{L}P = \mathbf{I} \cdot \nabla P = \mathbf{I} \cdot \left(\frac{\partial P}{\partial H_1}\nabla H_1 + \frac{\partial P}{\partial H_2}\nabla H_2\right) = \begin{pmatrix} 0 \\ 0 \\ 0 \end{pmatrix}\ . \tag{38}$$

(Above, we used again that $\mathbf{I} \cdot \nabla H_1 = 0$ and $\mathbf{I} \cdot \nabla H_2 = 0$ holds.) Consequently, in case IV ($b_1, b_2 > 0$) if we follow the limit cycle of the deterministic system ($Q = 0$) then the stationary probability density P defined by Eq. (34) does not change along that limit cycle. This indicates that P is maximal along the closed orbit defined in the phase space (x, v_1, v_2) that corresponds to the deterministic limit cycle for any given parameter set $a, b_1, b_2 > 0$.

4 Conclusions

The harmonic oscillator and the rigid body rotator are two fundamental systems of classical mechanics. However, the oscillatory motions of these systems are of different types. The oscillation of the harmonic oscillator emerges from the interplay between an inertia force and a restoring force that acts in the direction of the oscillator motion. In contrast, the oscillation of a mass point of a rotation emerges form the interplay of the inertia of that mass point and a constraint force that acts orthogonal to the motion of the mass point. In previous studies, classical rotator systems have been studied in the framework of Nambu mechanics and have been generalized to describe active rotators that are subjected to pumping and damping [32,33]. In contrast, in the present study, the Yamaleev oscillator has been studied that can be considered as a generalized harmonic oscillator involving a restoring force. Consequently, in the present study, we have highlighted a different aspect of oscillatory nonequilibrium Nambu systems.

The equilibrium oscillator originally proposed by Yamaleev involves two invariants, H_1 and H_2, that are composed of two kinetic energy variables $T_1 = v_1^2/2$ and $T_2 = v_2^2/2$ and one potential energy variable $V = ax^2/2$. Oscillations are characterized by an exchange of energy between T_1, T_2, and V. In the case of the nonequilibrium version of the Yamaleev oscillator the variables H_1 and H_2 in general vary as functions of time t. In the deterministic case, they either increase or decrease monotonically during transient periods (see Sec. 3.1.1. e.g., Eq. (18)). Eventually they converge to fixed point values. If both pumping parameters b_1 and b_2 are positive then the nonequilibrium oscillator approaches a stable limit cycle. On that limit cycle, the system dynamics is characterized again by the aforementioned exchange between the energy forms: T_1, T_2, and V. That is, while H_1 and H_2 are invariants of motion on the limit cycle, the functions T_1, T_2, and V are not.

In Sec. 3.3 we have demonstrated that the stochastic behavior of the nonequilibrium Yamaleev oscillator ($Q > 0$) reflects the deterministic properties of the oscillator ($Q = 0$) discussed in Sections 3.1 and 3.2. We showed that the probability density of the oscillator for $Q > 0$ becomes maximal at the stable limit cycles and stable fixed points that can be observed for $Q = 0$.

As argued above, the Yamaleev oscillator is an important model-system for our understanding of oscillatory nonequilibrium Nambu systems because (as opposed to previously studied Nambu rotator systems) the Yamaleev oscillator involves a generalized restoring force and features the exchange between different energy forms. In addition, the Yamaleev oscillator and its generalization as discussed in our study may be of interest for various other reasons.

First, it has been argued that the dynamical properties of the Yamaleev oscillator reflect the dynamical properties of a relativistic particle subjected to a spring-like linear restoring force [18,19]. More precisely, for certain initial conditions $(x(0), v_1(0), v_2(0))$ we can map by means of appropriate variable transformations in space and time solutions of the Yamaleev oscillator (6) to the solutions of the relativistic harmonic oscillator (see Appendix 5.2). In this context, we also note that for the both systems, i.e., for relativistic oscillator and for the Yamaleev oscillator (6), exact solutions can be found in terms of Jacobian elliptic functions [18,19,36].

Second, from Eq. (6) it follows that the oscillator dynamics can be cast into the form

$$\frac{\mathrm{d}^2}{\mathrm{d}t^2}\, x = -2ax \underbrace{(H_1 + H_2 - ax^2)}_{U(t)} = -\frac{\mathrm{d}V(x)}{\mathrm{d}x} \tag{39}$$

with

$$V = a(H_1 + H_2)x - \frac{a^2x^4}{2} \tag{40}$$

(see also [18,34]). Here, $H_1, H_2 \geq 0$ are considered as oscillator parameters. The initial elongation $x(0)$ is subjected to the constraints $ax(0)^2 < 2H_1$ and $ax(0)^2 < 2H_2$, while the initial velocity dx/dt is given by $dx/dt = \pm\sqrt{(2H_1 - ax(0)^2)(2H_2 - ax(0)^2)}$. That is, we are dealing with an anharmonic oscillator that exhibits a particular initial velocity and an attractive force decaying with distance from the origin $x = 0$. Such potential forces that become weaker with distance play an important role in solid state physics (e.g. Morse potential). Recall that $U(t) = H_1 + H_2 - ax^2(t) \geq 0$ holds for all $t \geq 0$ when following the trajectory of the Yamaleev oscillator in the original three-dimensional space (x, v_1, v_2). Consequently, the oscillator cannot escape the basin of attraction of the origin and oscillations are bounded. This observation is consistent with the discussions made in Sec. 2.

Our study also sheds a new light to the engineering problem to construct a dynamical system that evolves on a pre-defined limit cycle. For example, the deterministic, nonequilibrium Yamaleev oscillator defined by Eq. (11) ($\gamma > 0$ but $Q = 0$) solves the problem to find a dynamical system that evolves on a stable limit cycle in the three-dimensional space (x, v_1, v_2), where the limit cycle is defined by the intersection of hypersurfaces given in terms of the constraints $H_1 = b_1$ and $H_2 = b_2$. This has been graphically illustrated by Figs. 1,...,3. Note that the Nambu dynamics pre-defines a particular temporal evolution on the limit cycle. However, we can modify this evolution by generalizing Eq. (11) for $Q = 0$ by introducing a state-dependent factor ω that determines the rate of change of the state vector $\mathbf{r}$. That is, for the purpose of defining a more general type of limit cycle oscillator, Eq. (11) may be replaced by

$$\frac{\mathrm{d}}{\mathrm{d}t}\mathbf{r} = \omega(\mathbf{r})\nabla H_1 \times \nabla H_2 - \nabla_D\, g\ . \tag{41}$$

In fact, nature seems to take advantage of dynamical systems of this kind at least for $g = 0$ because biochemical reaction equations can be cast into the form (41) with $\omega \neq 0$ (for details see [16,17]). Future research may be directed to explore in more detail potential benefits of constructing limit cycles dynamics using generalizations of the nonequilibrium Yamaleev oscillator introduced in Sec. 3.

Acknowledgments

TDF acknowledges funding by an award from Science Foundation Ireland (SFI) reference number: 06/CE/B1129

5 Appendix

5.1 Appendix A: stability analysis of the fixed point $(x \neq 0,0,0)$ for the case $b_1 > 0 \wedge b_2 > 0$

We consider first the case $b_1 \neq b_2$. Then for the fixed point $(x \neq 0,0,0)$ we either have $ax^2/2 \neq b_1$ or $ax^2/2 \neq b_2$. Let us assume $ax^2/2 \neq b_1$ (the case $ax^2/2 \neq b_2$ can be treated by analogy). The idea then is that a perturbation of H_1 in the direction of b_1 will not decay because H_1 as long as $v_1 \neq 0$ tends to approach the value b_1, see Eq. (18). In line with this idea, we note that the unperturbed Hamiltonian function H_1 is $H_1 = ax^2/2$. Let $H_1(0)$ denote the perturbed function involving $x(0) \approx x$ but $x(0) \neq x$ and $v_1(0) \approx 0$ but $v_1(0) \neq 0$, i.e., $v_1(0)$ is a small, finite number. We put $x(0) = x - \epsilon$, where ϵ is a small number. We choose ϵ and $v_1(0)$ such that $|H_1(0) - b_1| < |H_1 - b_1|$. That is, the perturbed Hamiltonian $H_1(0)$ is "closer" to b_1 then the unperturbed Hamiltonian H_1. Let us assume that $b_1 < ax^2/2$ (we can treat the other case similar). Then we need a perturbation of H_1 such that $H_1(0) < ax^2/2$. We have $H_1(0) = v_1(0)^2/2 + ax(0)^2/2$ and we require that the inequality $H_1(0) < H_1 = ax^2/2$ holds. Substituting $x(0) = x - \epsilon$ into this inequality yields $v_1(0)^2 < \epsilon(2x - a\epsilon)$. Consequently, if we consider a perturbation composed of the pair $(v_1(0), \epsilon)$ satisfying this constraint then we have $b_1 < H_1(0) < H_1$. From Eq. (18) it follows that in general the difference $|H_1(t) - b_1|$ can only decrease as long as $v_1 \neq 0$. Consequently, the perturbation with the initial condition $(v_1(0), x(0) = x - \epsilon)$ evolves in such a way that $|H_1(t) - b_1| < |H_1 - b_1|$ for all times. The dynamical system cannot evolve to the unperturbed state, which means that $(x \neq 0,0,0)$ represents an unstable fixed point.

Next, we consider the special case $b_1 = b_2 = b > 0$. We first focus on fixed points $(x \neq 0,0,0)$ with $ax^2/2 \neq b$. If this assumption holds then we can use the same line of argument made above for the case $b_1 \neq b_2$. If $ax^2/2 \neq b$ then we consider a perturbation with initial value $H_1(0)$ such that the difference $|H_1(0) - b|$ is smaller than the difference $|H_1 - b|$ of the unperturbed case.

Finally, we have to consider the case $b_1 = b_2 = b > 0$ for $(x \neq 0,0,0)$ with $ax^2/2 = b$. That is, we have $x = \pm\sqrt{2b/a}$ and the fixed point reads explicitly $(\pm\sqrt{2b/a}, 0, 0)$. The Hamiltonian functions at that fixed point are $H_1 = H_2 = b$. Consequently, close to $(\pm\sqrt{2b/a}, 0, 0)$ the expression $v_1(H_1 - b_1)$ and $v_2(H_2 - b_2)$ occurring in Eq. (14) are small quantities of second order. Linearizing Eq. (14) at $(\pm\sqrt{2b/a}, 0, 0)$ yields the evolution equations $\mathrm{d}v_1/\mathrm{d}t = -av_2x$ and $\mathrm{d}v_2/\mathrm{d}t = -av_1x$ where x is a constant with $x = \pm\sqrt{2b/a}$. From these equations we obtain the second-order differential equation $\mathrm{d}^2v_1/\mathrm{d}t^2 = (ax)^2v_1 = 2abv_1$, which describes an unstable dynamical system. We arrive again at the conclusion that the fixed point $(x \neq 0,0,0)$ is unstable.

5.2 Appendix B: relativistic harmonic oscillator

Detailed discussions on the link between the Yamaleev oscillator and the relativistic harmonic oscillator can be found in [18,19,34]. We briefly sketch here the link between the Yamaleev model (6) and the relativistic harmonic oscillator. In the context of the relativistic harmonic oscillator, we first note that the Yamaleev oscillator describes the oscillator dynamics in the proper time (eigentime) of the oscillator rescaled by a mass-related factor m. We will denote by this time by s. In our case $m = 1/2$. That is, the departure point is the coupled set of equations

$$\frac{\mathrm{d}x(s)}{\mathrm{d}s} = v_1v_2 \ , \frac{\mathrm{d}v_1(s)}{\mathrm{d}s} = -axv_2 \ , \frac{\mathrm{d}v_2(s)}{\mathrm{d}s} = -axv_1 \quad (42)$$

rather than the model described by Eq. (6). We map next $(x(s), v_1(s), v_2(s))$ to the variables $(x(s), p_0(s), p(s))$ (using the notation suggested in [19]), where p_0 and p will later be interpreted as Lorentz factor and the relativistic moment, respectively. At this stage of our derivation, however, $p_0(s)$ and $p(s)$ are defined by

$$p_0 = \frac{v_1^2 + v_2^2}{4} \ , \ p = \frac{v_1v_2}{2} \ . \quad (43)$$

From Eq. (42) it follows that

$$\frac{\mathrm{d}x(s)}{\mathrm{d}s} = 2p \ , \frac{\mathrm{d}p_0(s)}{\mathrm{d}s} = -2axp \ , \frac{\mathrm{d}p(s)}{\mathrm{d}s} = -2axp_0 \ , \quad (44)$$

which implies that $p_0^2(s) - p^2(s) = C$ is an invariant as indicated by the constant C. We require next that only initial conditions $x(0), v_1(0), v_2(0)$ are considered such that $C = 1$ holds (e.g., for $v_1(0) = 2$ and $v_2(0) = 0$ we obtain $p_0(0) = 1$, $p(0) = 0$, and $C = 1$). Subsequently, we consider the variables $x(s), p_0(s), p(s)$ from the laboratory system such that they are measured in the relativistic time t (laboratory time): $x(t), p_0(t), p(t)$. The time transformation $s \to t$ reads $\mathrm{d}s/m = \sqrt{1 - v^2(t)}\mathrm{d}t$ with $v(t) = \mathrm{d}x/\mathrm{d}t$. The factor m is the aforementioned mass-like factor related to the re-scaled proper time s. From Eq. (44) it follows that

$$p(t) = \frac{v(t)}{\sqrt{1 - v(t)^2}} \ . \quad (45)$$

Note that for sake of conveniency we have put in our derivation the speed of the light equal to unity. From $p_0^2 - p^2 = 1$ it follows $p_0(t) = 1/\sqrt{1 - v^2(t)}$ (Lorentz factor) such that the time-transformation $s \to t$ actually reads $\mathrm{d}t = (p_0/m)\mathrm{d}s$, see [19]. Finally, differentiating Eq. (45) with respect to t and exploiting the result $p_0(t) = 1/\sqrt{1 - v^2(t)}$ and Eq. (44), we obtain

$$\frac{\mathrm{d}}{\mathrm{d}t}p(t) = -ax(t) \ . \quad (46)$$

Equations (45,46) describe the relativistic harmonic oscillator (speed of light equal to unity and rest mass equal to unity) and may be written like

$$\frac{\mathrm{d}}{\mathrm{d}t}\frac{v(t)}{\sqrt{1 - v^2(t)}} = -ax(t) \ , \ \frac{\mathrm{d}}{\mathrm{d}t}x = v \ . \quad (47)$$

References

1. Y. Nambu, Phys. Rev. D **7**, 2405 (1973).
2. S. A. Pandit and A. D. Gangal, J. Phys. A **31**, 2899 (1998).
3. A. R. Plastino, A. Plastino, L. R. da Silva, and M. Casas, Physica A **271**, 343 (1999).
4. G. B. Roston, A. R. Plastino, M. Casas, A. Plastino, and L. R. da Silva, Eur. Phys. J. B **48**, 87 (2005).
5. W. H. Steeb and N. Euler, Il Nuovo Cimento **106B**, 263 (1991).
6. A. Tegmen, Czech. J. Phys. **54**, 749 (2004).
7. D. Baleanu, Proc. Inst. Math. NAS of Ukraine **50(2)**, 611 (2004).
8. T. L. Curtright and C. Zachos, New J. Phys. **4**, 83.1 (2002).
9. T. L. Curtright and C. Zachos, Phys. Rev. D **68**, 085001 (2002).
10. C. Zachos, Phys. Lett. B **570**, 82 (2003).
11. S. Codriansky, C. A. G. Bernardo, A. Aglaee, F. Carrillo, J. Castellanos, G. Pereira, and J. Perez, J. Phys. A **27**, 2565 (1994).
12. M. Hirayama, Phys. Rev. D **16**, 530 (1977).
13. A. R. Plastino and A. Plastino, Physica A **232**, 458 (1996).
14. N. G. Pletnev, Siberian Electronic Mathematical Reports **6**, 272 (2009).
15. R. M. Yamaleev, Annals of Phys. N.Y. **292**, 157 (2001).
16. T. D. Frank, J. Biol. Phys. **37**, 375 (2011).
17. T. D. Frank, J. Nonlin. Math. Phys. (in press), Nambu brackt formulation of nonlinear biochemical reactions beyond elementary mass action kinetics.
18. R. M. Yamaleev, Annals of Phys. N.Y. **277**, 1 (1999).
19. R. M. Yamaleev, Annals of Phys. N.Y. **285**, 141 (2000).
20. C. Gonera and Y. Nuktu, Phys. Lett. A **285**, 301 (2001).
21. A. Tegmen and A. Vercin, Int. J. Mod. Phys. B **19**, 393 (2004).
22. F. Schweitzer, *Brownian agents and active particles* (Springer, Berlin, 2003).
23. H. Haken, Z. Physik **263**, 267 (1973).
24. M. Hongler and D. M. Ryter, Z. Physik B **31**, 333 (1978).
25. W. Ebeling and I. M. Sokolov, *Statistical thermodynamics and stochastic theory of nonequilibrium systems* (World Scientific, Singapore, 2004).
26. U. Erdmann, W. Ebeling, and A. Mikhailov, Phys. Rev. E **71**, 051904 (2005).
27. W. Ebeling and L. Schimansky-Geier, Eur. Phys. J. ST **157**, 17 (2008).
28. W. Ebeling, F. Schweitzer, and B. Tilch, BioSystems **49**, 17 (1999).
29. B. Lindner and E. M. Nicola, Eur. Phys. J. ST **157**, 43 (2008).
30. A. Czirok, A. L. Barabasi, and T. Vicsek, Phys. Rev. Lett. **82**, 209 (1999).
31. J. W. Rayleigh, *Theory of sound* (Dover, New York, 1945), first edition published 1894.
32. T. D. Frank, Eur. Phys. J. B **74**, 195 (2010).
33. T. D. Frank, Phys. Lett. A **374**, 3136 (2010).
34. A. Molgado and A. Rodriguez, J. Nonlin. Math. Phys. **14**, 534 (2007).
35. H. Risken, *The Fokker-Planck equation — Methods of solution and applications* (Springer, Berlin, 1989).
36. A. L. Harvey, Phys. Rev. D **6**, 1474 (1972).